Journal of Solid State Chemistry 184 (2011) 1129–1134

Contents lists available at ScienceDirect

Journal of Solid State Chemistry

journal homepage: www.elsevier.com/locate/jssc

Magnetic behavior of $MnPS_3$ phases intercalated by $[Zn_2L]^{2+}$ (LH_2: macrocyclic ligand obtained by condensation of 2-hydroxy-5-methyl-1,3-benzenedicarbaldehyde and 1,2-diaminobenzene)

E. Spodine [a,b,*], P. Valencia-Gálvez [b,c], P. Fuentealba [a,b], J. Manzur [b,c], D. Ruiz [a], D. Venegas-Yazigi [b,d], V. Paredes-García [b,e], R. Cardoso-Gil [f], W. Schnelle [f], R. Kniep [f]

[a] Facultad de Ciencias Químicas y Farmacéuticas, Universidad de Chile, Chile
[b] Centro para el Desarrollo de Nanociencia y Nanotecnología, Cedenna, Chile
[c] Facultad de Ciencias Físicas y Matemáticas, Universidad de Chile, Chile
[d] Facultad de Química y Biología, Universidad de Santiago de Chile, Chile
[e] Departamento de Química, Universidad Tecnológica Metropolitana, Chile
[f] Max-Planck-Institut fur Chemische Physik fester Stoffe, Germany

ARTICLE INFO

Article history:
Received 13 September 2010
Received in revised form
27 January 2011
Accepted 3 March 2011
Available online 21 March 2011

Keywords:
Intercalated $MnPS_3$ phase
Binuclear Zn(II) macrocyclic complex
Magnetic properties
Microwave assisted synthesis

ABSTRACT

The intercalation of the cationic binuclear macrocyclic complex $[Zn_2L]^{2+}$ (LH_2: macrocyclic ligand obtained by the template condensation of 2-hydroxy-5-methyl-1,3-benzenedicarbaldehyde and 1,2-diaminobenzene) was achieved by a cationic exchange process, using $K_{0.4}Mn_{0.8}PS_3$ as a precursor. Three intercalated materials were obtained and characterized: $(Zn_2L)_{0.05}K_{0.3}Mn_{0.8}PS_3$ **(1)**, $(Zn_2L)_{0.1}K_{0.2}Mn_{0.8}PS_3$ **(2)** and $(Zn_2L)_{0.05}K_{0.3}Mn_{0.8}PS_3$ **(3)**, the latter phase being obtained by an assisted microwave radiation process. The magnetic data permit to estimate the Weiss temperature θ of ≈ -130 K for **(1)**; ≈ -155 K for **(2)** and ≈ -130 K for **(3)**. The spin canting present in the potassium precursor remains unperturbed in composite **(3)**, and spontaneous magnetization is observed under 50 K in both materials. However composites **(1)** and **(2)** do not present this spontaneous magnetization at low temperatures.

The electronic properties of the intercalates do not appear to be significantly altered. The reflectance spectra of the intercalated phases **(1)**, **(2)** and **(3)** show a gap value between 1.90 and 1.80 eV, lower than the value observed for the $K_{0.4}Mn_{0.8}PS_3$ precursor of 2.8 eV.

1. Introduction

The study of materials with lamellar structure has been generating a great interest over the past years due to their anisotropic physical properties. Materials with such a lamellar structure permit to host a wide range of guests, such as organic compounds [1,2], organometallics [3], polymers [4,5], and monovalent and trivalent cations [6–9]. This intercalation chemistry allows to obtain new materials in which the host properties are significantly modified. For example, nonlinear optic materials [1,9,10], magnetic materials [3,11,12], catalysts [13], electroactive materials [14], multifunctional [15,16] and new dielectric materials [17,18] are obtained by the intercalation of one of the above mentioned guests.

Transition-metal thiophosphate MPS_3, (M=Mn, Cd) present an inorganic lamellar structure, which can be described by analogy to the layered structure of the $CdCl_2$ type [19–21]. The electric and magnetic properties reported for $MnPS_3$ and $CdPS_3$ indicate a semiconductor character with low values of conductivity [22], and antiferromagnetic and diamagnetic properties, respectively [23]. The manganese and cadmium chalcogenides MPS_3 allow intercalation of voluminous guests through a cationic transfer processes followed by a cationic exchange [3,24].

An alternative synthetic route in order to obtain these compounds is the intercalation assisted by microwave radiation. This synthetic approach is largely used in organic chemistry, for example, in esterification, hydrolysis, and substitution reactions [25]. However, this alternative synthetic method is less used in inorganic reactions, except for reports for the use of microwaves in the intercalation of organic species in V_2O_5 [26], in the mixed oxide α-$VO(PO_4)$ [27], in $FePS_3$ and in $Fe_{0.86}Mn_{0.18}PS_3$ [28]. For the intercalation of coordination compounds in lamellar materials, literature reports the composites formed by Mn(III), Fe(III), and

* Corresponding author at: Facultad de Ciencias Químicas y Farmacéuticas, Universidad de Chile, Chile.
E-mail address: espodine@uchile.cl (E. Spodine).

0022-4596/$ - see front matter © 2011 Elsevier Inc. All rights reserved.
doi:10.1016/j.jssc.2011.03.009

Co(III) salen complexes with $MnPS_3$ (salen: Schiff base ligand derived from the condensation of salicylaldehyde and ethylenediamine) [3], by Fe(III) 5-MeO-sal$_2$trien complexes with $MnPS_3$ [29], by Fe(III) salen complexes with $CdPS_3$ [30], and by the sulfonatosalen Mn(III) complex with a zinc aluminum LDH host [31], among others.

From the magnetic point of view, $MnPS_3$ is an isotropic phase and contains a paramagnetic Mn(II) ion ($S=5/2$) coupled antiferromagnetically to the three nearest neighbors in the layer, and shows normal two-dimensional antiferromagnetism with a Néel temperature of 78 K [32]. These magnetic properties can be drastically modified by intercalation. For example, some $MnPS_3$ intercalates exhibit bulk spontaneous magnetization with a Curie temperature of 35–40 K [33–35].

This paper presents the study of the structural and property changes due to the intercalation of $[Zn_2L]^{2+}$ in the $MnPS_3$ phase (LH_2: macrocyclic ligand obtained by the template condensation of 2-hydroxy-5-methyl-1,3-benzenedicarbaldehyde and 1,2-diaminobenzene). Solid reflectance spectra and magnetic properties of the obtained composite materials are presented and discussed.

2. Experimental

2.1. Characterization

Infrared spectra of the powder samples were recorded in the 4000–400 cm^{-1} range at room temperature on a Bruker-IFS 28 spectrometer, using KBr pellets. Diffuse reflectance spectra were recorded on a Shimadzu UV-visible spectrophotometer, model 2450. The measurements were done on microcrystalline samples, which were dispersed between two polyethylene films supported on a $BaSO_4$ blank. The powder X-ray diffraction analysis was carried out using a difractometer with Cu-$K\alpha_1$ radiation, with an Imaging Plate Guinier Camera G 670, in the $5^\circ < 2\theta < 80^\circ$ range. Scanning electron microscopy (SEM) and energy dispersive X-ray spectroscopy (EDXS) analyses were done using a JOEL JEM 6400 equipment. The elemental composition was also determined with an ICP–OES Vista RL (VARIAN) analyzer, while the analysis of C, H and N was done with a LECO MICRO–CHNS–932 Analyzer

The magnetic properties were studied with a SQUID-magnetometer (MPMS XL7, Quantum Design); for the measurement a polycrystalline sample was filled into a pre-calibrated quartz tube. Susceptibility data were taken at 0.1 kOe in a temperature range of 1.8–400 K. The magnetization curve was recorded at 1.8 K, varying the external field from -10 to 10 kOe.

2.2. Synthesis of the $MnPS_3$ phase

Pure $MnPS_3$ was synthesized by the reaction of stoichiometric amounts of high purity elements in an evacuated quartz tube at 750 °C, as described in the literatures [19,20]. The X-ray diffraction pattern (Fig. 1S) was compared with the calculated one using the data given by Ouvrard et al. [19], showing the coincidence of the experimental and calculated peaks.

2.3. Preparation of the potassium intercalated precursor

$MnPS_3$ was treated with a 2 M aqueous solution of KCl for 24 h at room temperature using the conventional method, as described in the literatures [36,37]. After this intercalation process, the $K_{2x}Mn_{1-x}PS_3$ precursor was obtained with a stoichiometric composition of $K_{0.4}Mn_{0.8}PS_3$.

The intercalation was studied as a function of the size of the crystallites of the pristine $MnPS_3$. Suspensions of the pristine phase, with different crystallite size (100–80, 80–63, 63–40, 40–20 and $<20\,\mu m$) were filtered off after the intercalation process, and the intercalated solids were quantified for Mn(II). These results were compared with the EDXS analyses.

2.4. Synthesis of the macrocyclic complex $[Zn_2L](NO_3)_2$

The macrocyclic complex $[Zn_2L](NO_3)_2$ was prepared by the template method described in the literature [38]. The synthesis was achieved in two steps. Initially 2-hydroxy-5-methyl-1,3-benzenedicarbaldehyde was refluxed for 3 h with $Zn(NO_3)\cdot 4H_2O$ in 2-propanol, under a nitrogen atmosphere. After that 1,2-diaminobenzene dissolved in the same solvent was added to the reacting mixture and left to react at room temperature with stirring. A brick-red solid precipitated corresponding to $[Zn_2L](NO_3)_2$.

The precipitate was washed with acetone and methanol, and the purity of the isolated compound was verified by column chromatography. Anal. found (calcd.) C: 49.8% (49.68%); N: 11.2% (11.59%); H: 3.2% (3.06%); and Zn: 18.1% (18.04%).

2.5. Intercalation of the macrocyclic complex $[Zn_2L]^{2+}$

The intercalation of the macrocyclic zinc complex was done in two steps. First the potassium precursor was obtained by the cationic transfer process. This process consists of the intercalation of a monovalent cations (K^+) through the removal of the transition-metal (Mn^{2+}) ions from the layers, with consequent balance of the electrical charges. Then, in a second stage through cationic exchange, the monovalent cations were replaced by the new guest [20,21].

While the potassium precursor was obtained by the conventional method, in this work we present two synthetic methods for the preparation of the composites containing the macrocyclic complex: the conventional route, consisting of stirring the suspension for two and four weeks at room temperature, and the intercalation process assisted by microwave radiation.

2.5.1. Conventional intercalation of the cationic binuclear zinc macrocyclic complex

In an one-neck round bottom flask 300 mg of preintercalated $K_{0.4}Mn_{0.8}PS_3$ and 255 mg of $[Zn_2L](NO_3)_2$ were added to 25 mL of methanol, and stirred at room temperature for two and four weeks, respectively. $(Zn_2L)_{0.05}K_{0.3}Mn_{0.8}PS_3$ **(1)** was obtained after stirring for two weeks and $(Zn_2L)_{0.1}K_{0.2}Mn_{0.8}PS_3$ **(2)** after stirring four weeks. The dark red powders were filtered off, washed with methanol, and dried in an oven at 50 °C for two days. In order to eliminate any adsorbed complex, the composite was further purified by washing it several times with dimethylformamide, until the solvent remained colorless.

Intercalation reactions done for shorter time intervals did not give reproducible stoichiometries for the isolated composites. Therefore the composites obtained from the intercalation reaction done for two weeks of stirring were used for the magnetic characterization.

2.5.2. Intercalation of the cationic binuclear zinc macrocyclic complex assisted by microwave radiation

In a glass reaction vessel 300 mg of preintercalated $K_{0.4}Mn_{0.8}PS_3$ and 255 mg of $[Zn_2L](NO_3)_2$ were added to 25 mL methanol. The microwave irradiation of the suspension was carried out for 12 min with a microwave oven, LAVIS-1000 Multi-Quant of frequency 2459 MHz, with a power of 800 W. The time of irradiation was limited by the volatility of the solvent. $(Zn_2L)_{0.05}K_{0.3}Mn_{0.8}PS_3$ **(3)** was obtained and purified by a similar procedure as described in Section 2.5.1.

For both methods the nonexistence of adsorbed macrocyclic complex was verified by the absence of the vibration band of the ionic nitrate anion in the infrared spectrum.

3. Results and discussion

3.1. Preparation of the potassium precursor

Five analyzed samples, corresponding to particles of 100–80, 80–63, 63–40, 40–20 and <20 μm, gave the same concentration of manganese (II) ions being eliminated from the pristine phase, independent of the size of the particles. Therefore it was assumed that the potassium precursor phase, obtained after 24 h of intercalation process, could always be identified with the formula $K_{0.4}Mn_{0.8}PS_3$, independent of the size of the used particles. Further experiments were done using the powder of the $MnPS_3$ phase without any separation by particle size.

3.2. Intercalated phases with $[Zn_2L]^{2+}$

EDXS and ICP–OES results for **(1)**, **(2)**, and **(3)** were used to determine the Zn, Mn, P, S, and K composition in the intercalated samples. Both results show that the occurrence of full replacement of the macrocyclic zinc complex is not obtained, since potassium is still present in all the resulting composites. The comparison of the mean composition of the intercalated phases by the conventional and by the microwave-assisted methods shows that the microwave-assisted process gives the same composition as the two week conventional replacement process.

The X-ray diffraction on powder samples allows to identify the modification of the interlamellar space due to the intercalation process. Thus, this can be followed by analyzing the displacement of the (0 0 1) reflection. The increase of the interlamellar distance, from 9.4 Å for $K_{0.4}Mn_{0.8}PS_3$ to 10 Å for the composite containing the macrocyclic complex, can be observed for all the samples obtained by both intercalation methods (conventional and via microwave radiation). Fig. 1 shows the diffractograms for the composites obtained by the conventional intercalation method (2 and 4 weeks), and for the composite obtained by the intercalation process assisted by microwave radiation (12 min), compared with the precursor $K_{0.4}Mn_{0.8}PS_3$. Table 1 summarizes the values obtained for the interlamellar distance from the value of 2θ of the diffraction plane (0 0 1), for the intercalated, preintercalated and pure $MnPS_3$ phase.

According to the diffractograms the average interlamellar distance of the intercalated compounds **(1)**, **(2)**, and **(3)** is 10 Å. Therefore, the interlamellar distance with respect to the precursor phase ($K_{0.4}Mn_{0.8}PS_3$) is increased by approximately 0.6 Å, for all the intercalated composites. Two limiting intercalation positions of the guest in the lamellar $MnPS_3$ structure can be considered, one in which the macrocyclic complex is in the perpendicular position and the second one in which this species is parallel to the planes of the lamellar structure [39–41]. Assuming that the longest end-to-end distance in the macrocyclic complex corresponds to the carbon–carbon distance of the methyl substituents of the opposite phenol aromatic rings, this distance can be estimated approximately in 14 Å (Fig. 2). This assumption is made by taking crystallographic data of similar compounds [42,43]. The macrocyclic zinc complex $[Zn_2L'Cl_2]$ ($L'H_2$: macrocyclic ligand derived from 2-hydroxy-5-methyl-1,3-benzenedicarbaldehyde and 1,2-cyclohexanediamine), whose structure was determined by single-crystal X-ray diffraction [42], was used as model for the estimation of the interlayer distance. Since the interlamellar distance in the composite is 10 Å the perpendicular intercalation is not possible, and we propose that the zinc macrocyclic complex is intercalated between the layers in the parallel mode. This type

Table 1
Interlamellar distance for the pure phase, potassium precursor and intercalation compounds.

Phase	2θ (deg.)	d (Å)	Δd (Å) precursor—macrocyclic intercalate
$MnPS_3$	13.64	6.49	Not applicable
$K_{0.4}Mn_{0.8}PS_3$	9.40	9.41	Not applicable
$[Zn_2L]_{0.05}K_{0.3}Mn_{0.8}PS_3$	8.84	10.00	0.59
$[Zn_2L]_{0.1}K_{0.2}Mn_{0.8}PS_3$	8.78	10.07	0.66
$[Zn_2L]_{0.05}K_{0.3}Mn_{0.8}PS_3$	8.80	10.05	0.67

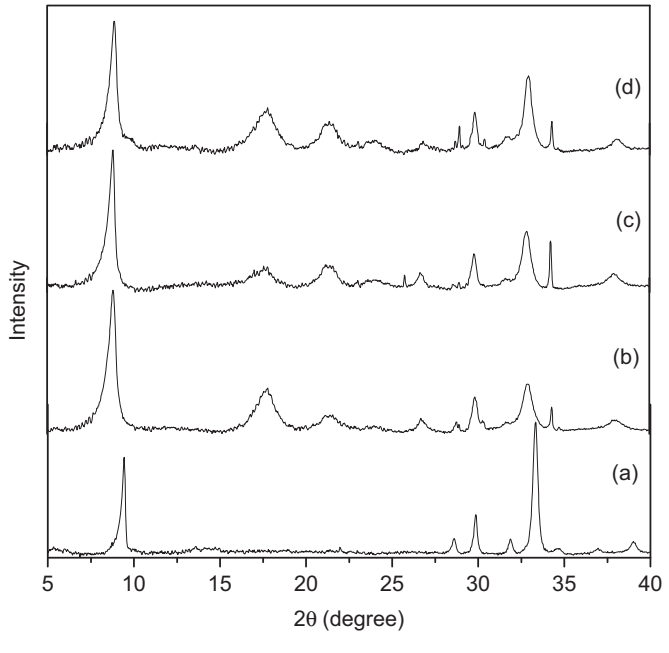

Fig. 1. XRD of (a) $K_{0.4}Mn_{0.8}PS_3$; (b) $[Zn_2L]_{0.05}K_{0.3}Mn_{0.8}PS_3$ **(1)**; (c) $[Zn_2L]_{0.1}K_{0.2}Mn_{0.8}PS_3$ **(2)**; and (d) $[Zn_2L]_{0.05}K_{0.3}Mn_{0.8}PS_3$ **(3)**.

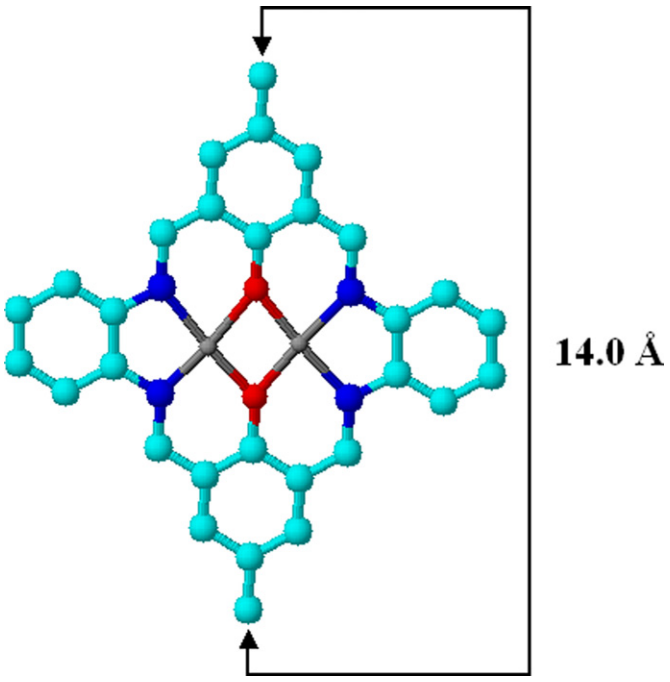

Fig. 2. Estimated end to end distance for the macrocyclic complex $[Zn_2L]^{2+}$.

of orientation also permits a better interaction of the aromatic system of the macrocyclic ligand with the layers.

The assignment of the IR bands for the guest $[Zn_2L]^{2+}$ and intercalated materials, obtained by both methods are summarized in Table 2. The intercalated compounds $[Zn_2L]_{0.05}K_{0.3}Mn_{0.8}PS_3$ **(1)**, $[Zn_2L]_{0.1}K_{0.2}Mn_{0.8}PS_3$ **(2)** and $[Zn_2L]_{0.05}K_{0.3}Mn_{0.8}PS_3$ **(3)**, obtained by the conventional and microwave assisted methods, show some characteristic bands of the macrocyclic complex, attributed to the stretching modes $\nu_{C=N}$, $\nu_{C=C}$ and ν_{C-H}, and also show the splitting of the stretching mode ν_{PS3} into three components at 609, 590 and 555 cm^{-1},respectively. The splitting of the asymmetric PS_3 vibration mode reflects the Mn^{2+} vacancies produced by the introduction of the potassium ions with the concomitant removal of manganese ions, and the presence of the intercalated macrocyclic complex [44]. The presence of the vibration bands attributed to the organic ligand of the guest molecule and the absence of the ionic nitrate band at 1384 cm^{-1} of the original macrocyclic complex can be used as indicative of the fact that the complex has been intercalated, and is not adsorbed on the lamellar phase.

3.3. Diffuse reflectance spectroscopy (DRS)

The diffuse reflectance spectra of the microcrystalline solids show that the observed gap for composites **(1)** and **(2)** is 1.90 eV (Fig. 2Sa,b), remaining constant independent of the amount of intercalated complex. The intercalate **(3)** (microwave-assisted synthesis) gave a slightly lower gap of 1.80 eV (Fig. 2Sc). Therefore it becomes evident that this last synthetic method gives an intercalated material whose physical properties are different from the ones observed for the intercalated species obtained by the microwave method. All three intercalted phases present a lower energy gap than the $K_{0.4}Mn_{0.8}PS_3$ precursor, which presents it at 2.8 eV (Fig. 2Sd).

3.4. Magnetic study

Figs. 3 and 4 show the temperature dependence of χT and χ^{-1} for the composites $[Zn_2L]_{0.05}K_{0.3}Mn_{0.8}PS_3$ **(1)**, $[Zn_2L]_{0.1}K_{0.2}Mn_{0.8}PS_3$ **(2)** and $[Zn_2L]_{0.05}K_{0.3}Mn_{0.8}PS_3$ **(3)**. The $\chi^{-1}(T)$ plots permit to determine the Weiss constant by extrapolation from the paramagnetic region for each set of data for the intercalated phases. The obtained values are: $\theta \approx -130$ K for **(1)**; $\theta \approx -155$ K for **(2)** and $\theta \approx -130$ K for **(3)**. These values are more negative than the value of the Weiss constant for the precursor $K_{0.4}Mn_{0.8}PS_3$ ($\theta \approx -100$ K). All the obtained values for the Weiss constant indicate that the interactions in the intercalated phases and potassium precursor are antiferromagnetic. The antiferromagnetic interactions of the potassium precursor and intercalated phases are greatly diminished, compared with the pristine phase $MnPS_3$ ($\theta = -260$ K). Neither the potassium precursor nor the composites, which contain the zinc macrocyclic complex, show the maximum in the susceptibility data, characteristic of the intralamellar antiferromagnetism of the pristine $MnPS_3$ phase.

The intercalated phase **(3)**, obtained via microwave radiation, presents the same sharp increase in the χT value in the low temperature range as the potassium precursor (Fig. 3). This sharp change in susceptibility suggests that these compounds have a

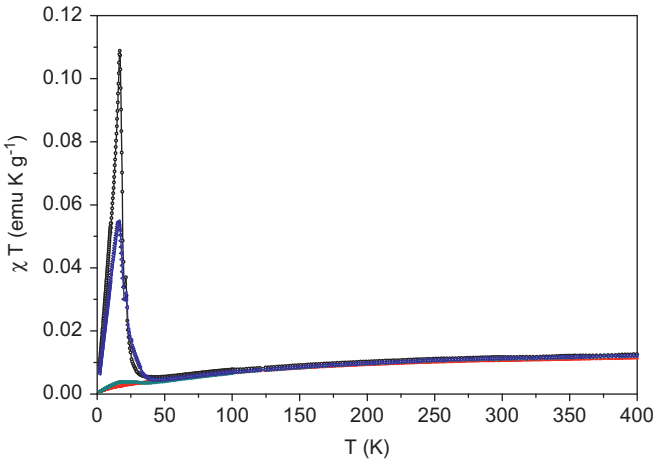

Fig. 3. Plot of χT(T) for $[Zn_2L]_{0.05}K_{0.3}Mn_{0.8}PS_3$ composite **(1)** (red); $[Zn_2L]_{0.1}K_{0.2}Mn_{0.8}PS_3$ composite **(2)** (cyan); $[Zn_2L]_{0.05}K_{0.3}Mn_{0.8}PS_3$ composite **(3)** (blue); and $K_{0.4}Mn_{0.8}PS_3$ (black). (For interpretation of the references to color in this figure legend, the reader is referred to the web version of this article.)

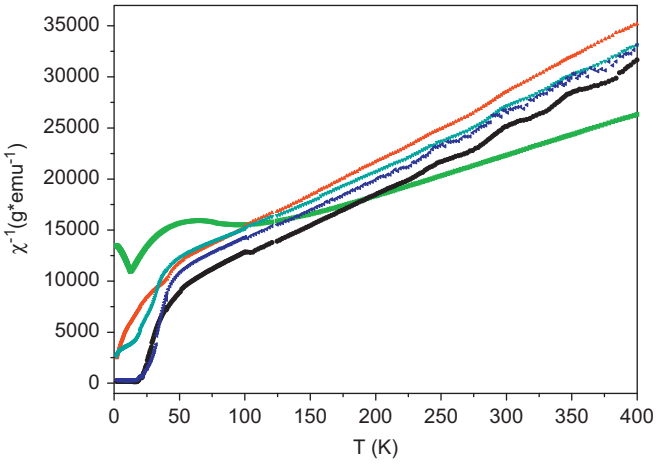

Fig. 4. Plot of χ^{-1}(T) for $[Zn_2L]_{0.05}K_{0.3}Mn_{0.8}PS_3$ composite **(1)** (red); $[Zn_2L]_{0.1}K_{0.2}Mn_{0.8}PS_3$ composite **(2)** (cyan); $[Zn_2L]_{0.05}K_{0.3}Mn_{0.8}PS_3$ **(3)** (blue); $K_{0.4}Mn_{0.8}PS_3$ (black); and $MnPS_3$ (green). (For interpretation of the references to color in this figure legend, the reader is referred to the web version of this article.)

Table 2
Comparison of IR data of the guest $[Zn_2L]\cdot(NO_3)_2$ with the intercalated compounds.

IR data	$[Zn_2L]\cdot(NO_3)_2$ (cm^{-1})	$[Zn_2L]_{0.05}K_{0.3}Mn_{0.8}PS_3$ **(1)**	$[Zn_2L]_{0.1}K_{0.2}Mn_{0.8}PS_3$ **(2)**	$[Zn_2L]_{0.05}K_{0.3}Mn_{0.8}PS_3$ **(3)**
νC=N	1618	1645	1646	1645
νC=C	1534	1533	1533	1533
$(NO_3)^-$	1384			
$\nu C-O_{Ph}$	1298			
νC–H	755	755	755	755
νPS_3		609	609	609
		590	590	590
		555	555	555
νP–P		447	447	447

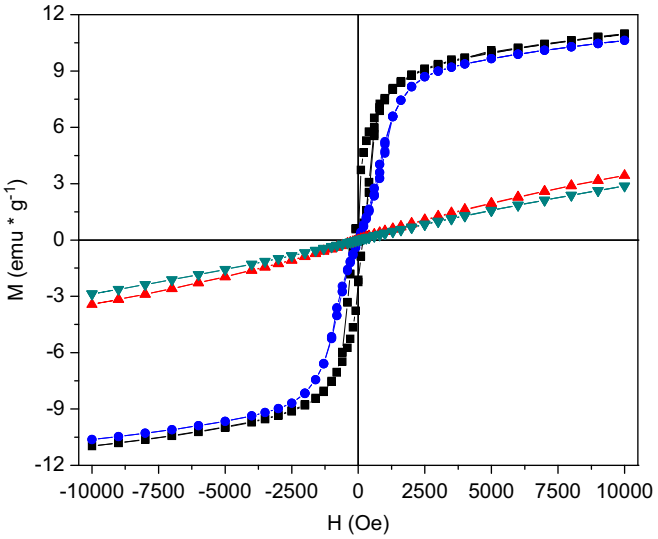

Fig. 5. Plot of M(H) at 1.8 K for $[Zn_2L]_{0.05}K_{0.3}Mn_{0.8}PS_3$ composite **(1)** (red); $[Zn_2L]_{0.1}K_{0.2}Mn_{0.8}PS_3$ composite **(2)** (cyan); $[Zn_2L]_{0.05}K_{0.3}Mn_{0.8}PS_3$ **(3)** (blue) and $K_{0.4}Mn_{0.8}PS_3$ (black). (For interpretation of the references to color in this figure legend, the reader is referred to the web version of this article.)

spontaneous magnetization under 50 K. However, such an increase was not detected for composites **(1)** and **(2)**, obtained by the conventional intercalation method (Fig. 3). Joy and Vasudevan [35] proposed a mechanism to explain the origin of the spontaneous magnetization for some $MnPS_3$ intercalates. They suggested that a canting of spins caused by the change in the local symmetry of a Mn(II) ion near the intralayered Mn(II) ion vacancy leads to weak long-range ferromagnetic order and spontaneous magnetization at low-temperature.

The magnetization curve at 1.8 K of **(1)**, **(2)** and **(3)** was done from -10 to $+10$ kOe, and an abrupt increase in the magnetization of **(3)** was observed at low values of magnetic field, up to 2.5 kOe (Fig. 5). The complete hysteresis loop was done at this same temperature, and is shown in the inset of Fig. 5. This behavior is also observed for the potassium precursor $K_{0.4}Mn_{0.8}PS_3$, while composites **(1)** and **(2)** present a paramagnetic behavior (Fig. 5).

Therefore, these results are indicating that if spin canting is assumed to be present in the potassium precursor and being responsible for the spontaneous magnetization [45], this phenomenon is also observed in the composite **(3)**, obtained by the microwave assisted intercalation reaction. It may be concluded that during the long period of time necessary for the intercalation reaction using the conventional method a subtle crystallographic change occurs, which perturbs somehow the local symmetry of the manganese centers in the $MnSP_3$ layers in such a way that the spin canting is no longer present, and therefore the magnetization is lost [4].

4. Final remarks

Two synthetic methods for the preparation of intercalated $MnSP_3$ with the zinc binuclear macrocyclic complex $[Zn_2L]^{2+}$ are reported. Even though both the conventional and the microwave assisted procedures permit to obtain composites with similar compositions, the physical properties result different. The magnetic behavior of the materials is different at low temperatures. $[Zn_2L]_{0.05}K_{0.3}Mn_{0.8}PS_3$ **(3)** displays a spontaneous magnetization as does the potassium precursor $K_{0.4}Mn_{0.8}PS_3$, a phenomenon which is not observed in the composites obtained by the conventional method.

Acknowledgments

The authors thank the financial support of FONDECYT GRANT 1080318; DFG/CONICYT International Program; and Basal Financial Support for Scientific and Technological Centers of Excellence, FB0807. P.V.G. thanks CONICYT for the Doctoral fellowship 21061162, and for the Doctoral Thesis Support fellowship 24090008; "Becas de estadías cortas de investigación de la Universidad de Chile".

Appendix A. Supplementary Information

Supplementary data associated with this article can be found in the online version at doi:10.1016/j.jssc.2011.03.009.

References

[1] I. Lagadic, P.G. Lacroix, R. Clément, Chem. Mater. 9 (1997) 2004–2012.
[2] T. Miyazaki, K. Ichimura, S. Matsuzaki, M. Sano, J. Phys. Chem. Solids 9 (1993) 1023–1026.
[3] X. Zhang, H. Zhou, X. Su, X. Chen, C. Yang, J. Qin, M. Inokuchi, J. Alloys Compd 432 (2007) 247–252.
[4] D. Zhang, J. Qin, K. Yakushi, Y. Nakazawa, K. Ichimura, Materials Science and Engineering A286 (2000) 183–187.
[5] N. Sukpirom, C. Oriakhi, M. Lerner, Mater. Res. Bull. 35 (2000) 325–331.
[6] L. Silipigni, G. Di Marco, G. Salvato, V. Grasso, Appl. Surf. Sci. 252 (2005)1998–2005 252 (2005).
[7] L. Silipigni, T. Quattrone, L. Schiro, V. Grasso, L. Monsù, G. De Luca, G. Salvato, J. Appl. Phys. 104 (2008) 123711–1–5.
[8] D. Ruiz-León, V. Manríquez, J. Kasaneva, R.E. Avila, Mater. Res. Bull. 37 (2002) 981–989.
[9] R. Clément, A. Léaustic, K. Marney, A.H. Francis, J. Lumin. 60&61 (1994) 355–358.
[10] E. Delahaye, N. Sandeau, Y. Tao, S. Brasselet, R. Clement, J. Phys. Chem. C 113 (2009) 9092–9100.
[11] X. Zhang, X. Su, X. Chen, J. Qin, M. Inokuchi, Microporous Mesoporous Mater. 108 (2008) 95–102.
[12] H.Q. Zhou, X. Su, X.A. Zhang, X.G. Chen, C.L. Yang, J.G. Qin, M. Inokuchi, Mater. Res. Bull. 41 (2006) 2161–2167.
[13] B.M. Choudary, S. Madhi, N.S. Chowdari, M.L. Kantam, B. Sreedhar, J. Am. Chem. Soc. 124 (2002) 14127–14136.
[14] Y.V. Kuzminskii, B.M. Voronin, N.N. Redin, J. Power Sources 55 (1995) 133–141.
[15] P.G. Lacroix, R. Clément, K. Nakatani, J. Zyss, I. Ledoux, Science 263 (1994) 658–660.
[16] M. Aoike, T. Masubuchi, E. Gonmori, Y. Kubota, T. Watanabe, Y. Takahashi, K. Takase, Y. Takano, J. Alloys Compd. 451 (2008) 470–472.
[17] L. Silipigni, L. Schiro, T. Anatrone, V. Grasso, G. Salvato, L.M. Scolano, G. De Luca, J. Appl. Phys. 105 (2009) 123703. doi:10.1063/1.3148271.
[18] L. Silipigni, L. Schiro, V. Grasso, G. Salvato, L.M. Scolaro, G. De Luca, Nuovo Cimento della Societa Italiana di Fisica 125 (2010) 539–545.
[19] G. Ouvrard, R. Brec, J. Rouxel, Mater. Res. Bull. 20 (1985) 1181–1189.
[20] Y. Mathey, R. Clement, C. Sourisseau, G. Lucazea, Inorg. Chem. 19 (1980) 2773–2779.
[21] F.S. Khumalo, H.P. Hughes, Phys. Rev. B 23 (1981) 5375–5383.
[22] V. Grasso, F. Neri, S. Santangelo, L. Silipigni, M. Piacentinis, J. Phys. Condens. Matter 1 (1989) 3337–3347.
[23] G. Le Flem, R. Brec, G. Ouvard, A. Louisy, J. Phys. Chem. Solids 5 (1982) 455–461.
[24] R. Clement in Hybrid Organic Inorganic Composites Symposium Series, Eds. J.E. Mark, C.Y.C. Lee, P.A. Bianconi, ACS Washington DC, 1995.
[25] S. Caddick, Tetrahedron 51 (1995) 10403–10432 (including cited references).
[26] A.Vadivel Murugan, Electrochim. Acta 50 (2005) 4627–4636.
[27] K. Chatakandu, M. Green, D. Mingos, S. Reynolds, M. J. Chem. Soc. Chem. Commun. (1989) 1515–1517.
[28] L. Lomas, L. Azcue, G. Negrón, J. Flores, R. Clément, Revista de la Sociedad Química de México 44 (2000) 112–115.
[29] S. Floquet, S. Salunke, M. Boillot, R. Clement, F. Varret, K. Boukheddaden, E. Riviere, Chem. Mater. 14 (2002) 4164–4171.
[30] C.N. Field, M.L. Boillot, R. Clement, J. Mater. Chem. 8 (1998) 283–284.
[31] S. Bhattacharjee, J.A. Anderson, Chem. Commun. (2004) 554–555.
[32] W. Toyoshima, T. Masubuchi, T. Watanabe, K. Takase, K. Matsubayashi, Y. Uwatoko, Y. Takano, J. Phys.: Conf. 150 (2009) 042215.
[33] S.J. Price, D. O'Hara, R.J. Francis, A. Fogg, S. O'Brien, Chem. Commun. (1996) 2453–2454.

[34] J. Qin, C. Yang, K. Yakushi, Y. Nakazawa, K. Ichimura, Solid State Commun. 100 (1996) 427–431.
[35] P. Joy, S. Vasudevan, Phys. Rev. B 46 (1992) 5425–5433.
[36] R. Clement, J. Chem. Soc. Chem. Commun. (1980) 647–648.
[37] R. Clement, O. Garnier, J. Jegoudez, Inorg. Chem. 25 (1986) 1404–1409.
[38] V. Paredes-García, D. Venegas-Yazigi, A. Cabrera, P. Valencia-Gálvez, M. Arriagada, D. Ruiz-León, N. Pizarro, A. Zanocco, E. Spodine, Polyhedron 28 (2009) 2335–2340.
[39] A.A. El-Meligi, Mater. Chem. Phys. 89 (2005) 253–259.
[40] H.Q. Zhou, X. Su, X.G. Chen, M. Inouchi, D.Q. Zhang, J.G. Qin, Chin. J. Inorg. Chem. 24 (2008) 1261–1264.
[41] H.Q. Zhou, L. Zou, X.G. Chen, C.L. Yang, M. Inokuchi, J.G. Qin, J. Inclusion Phenom. Macrocyclic Chem. 62 (2008) 293–296.
[42] S.R. Korupoju, N. Mangayarkarasi, S. Ameerunisha, E.J. Valente, P.S. Zacharias, J. Chem. Soc., Dalton Trans. (2000) 2845–2852.
[43] J. Gao, Y.-G. Liu, Y. Zhou, L.M. Boxer, F.R. Woolley, R.A. Zingaro, Chem. Bio. Chem. 8 (2007) 332–340.
[44] A.A. El-Meligi, Mater. Chem. Phys. 84 (2004) 331–340.
[45] Ch. Yang, X. Chen, J. Qin, K. Yakushi, Y. Nakazawa, K. Ichimura, J. Solids State Chem. 150 (2000) 281–285.